Two Modes of Linear Layer-by-Layer Growth of Nanoparticle−Polylectrolyte Multilayers and Different Interactions in the Layer-by-layer Deposition

John W. Ostrander, Arif A. Mamedov, and Nicholas A. Kotov*

Contribution from the Department of Chemistry, Oklahoma State University, Stillwater, Oklahoma 74078

Received August 8, 2000

Abstract: The structure of the multilayer assemblies of yttrium iron garnet nanoparticles (YIG) with polyelectrolytes was investigated with the emphasis on the control of the particle density in the adsorption layers. It was found that the growth of YIG films prepared by the layer-by-layer assembly can occur via two deposition modes: (1) sequential adsorption of densely packed adsorption layers (normal growth mode) and (2) in-plane growth of isolated particle domains (lateral expansion mode). Importantly, the dependence of the optical density on the number of deposition cycles remains linear in both cases. Microscopy results indicate that the origin of the lateral growth is in the interplay of particle/particle and particle/polyelectrolyte interactions rather than in a substrate effect. The lateral expansion mode is a general attribute of the layer-by-layer deposition and can be observed for various aqueous colloids. For the preparation of sophisticated multifunctional assemblies on nanoparticles, the film growth via domain expansion should be avoided, and therefore, one must be able to control the growth pattern. The switch from lateral to normal growth mode can be effected by grafting charged organic groups to YIG nanoparticles. Hydrophobic interactions between the hydrocarbon groups of the modified YIG and polyelectrolyte significantly increase the attractive component of the particle/polyelectrolyte and particle/particle interactions. The films from modified YIG display densely packed nanoparticle layers with a greatly reduced number of defects.

Introduction

Advanced materials from inorganic nanoparticles are currently one of the most dynamic areas of today's science. They represent significant fundamental and commercial interest with a wide range of applications including the next generation optics, electronics, and sensors.[1] Synthetic methods of colloidal chemistry afford manipulation of their size, surface structure, and hence their properties.[2] In optical, electrical and magnetic devices, nanoparticles will be mostly used in the form of thin films. Currently, such films are typically made by spin coating,[3,4] spraying,[5,6] or sometimes simple painting[7] nanoparticle−matrix mixtures. The layer-by-layer assembly (LBL) developed by G. Decher is one of the most perspective new methods of thin film deposition, which was often used for oppositely charged polymers.[8−10] Recently, it has also been successfully applied to thin films of nanoparticles and various other inorganic materials.[11−33] Its simplicity and universality combined with the high quality of coatings and uniform distribution of nanoparticles opens broad perspectives for this technique both in research and in industry. Importantly, the LBL prevents phase segregation of a nanoparticles/polymer mixture, which often occurs for other methods,[3,4,34] and is detrimental for many applications. LBL can also significantly improve the accuracy of thin film deposition and lead to the production of stratified films with alternating layers of different substances of organic or inorganic nature which was demonstrated in our previous works.[11a,26]

(1) Klein, D. L.; Roth, R.; Lim, A. K. L.; Alivisatos, A. P.; McEuen, P. L. *Nature* **1997**, *389*, 699−701. Alivisatos, A. P. *J. Phys. Chem.* **1996**, *100*, 13226. Levy, B. *J. Electroceram.* **1997**, *1*, 239−272. Jose-Yacaman, M.; Mehl, R. F. *Met. Mater. Trans. A* **1998**, *29*, 713−725. Zhdanov, V. P.; Kasemo, B. *Appl. Surf. Sci.* **1998**, *135*, 297−306. Bacsa, R. R.; Kiwi, J. *Appl. Catal. B−Environ.* **1998**, *16*, 19−29. Serpone, N.; Lawless, D.; Disdier, J.; Herrmann, J.-M. *Langmuir* **1994**, *10*, 643−652. Bruchez, M., Jr.; Moronne, M.; Gin, P.; Weiss, S.; Alivisatos, A. P. *Science* **1998**, *281*, 2013−2016. Chan, W. C. W.; Nie, S. *Science* **1998**, *281*, 2016−2018.

(2) Alivisatos, A. P. *Science* **1996**, *271*, 933−937.

(3) Skandan, G. In Gonsalves, K. E., Baraton, M. I., Singh, R., Hofmann, H., Chen, J. X., Akkara, J. A., Eds.; Materials Research S: Warrendale, 1998; p. 351−362. De, G. T. *J. Sol.-Gel. Sci. Technol.* **1998**, *11*, 289−298. Chauhan, P.; Annapoorni, S.; Trikha, S. K. *Bull. Mater. Sci.* **1998**, *21*, 381−385.

(4) Chevreau, A.; Phillips, B.; Higgins, B. G.; Risbud, S. H. *J. Mater. Chem.* **1996**, *6*, 1643−1647. Fan, H.; Zhou, Y.; Lopez, G. P. *Adv. Mater. (Weinheim, Germany)* **1997**, *9*, 728−731. Fritzsche, W.; Porwol, H.; Wiegand, A.; Bornmann, S.; Kohler, J. M. *Nanostruct. Mater.* **1998**, *10*, 89−97. Lakhwani, S.; Rahaman, M. N. *J. Mater. Sci.* **1999**, *34*, 3909−3912. Barnes, K. A.; Karim, A.; Douglas, J. F.; Nakatani, A. I.; Gruell, H.; Amis, E. J. *Macromolecules* **2000**, *33*, 4177−4185.

(5) Salata, O. V.; Dobson, P. J.; Hull, P. J.; Hutchison, J. L. *Thin Solid Films* **1994**, *251*, 1−3. Salata, O. V.; Dobson, P. J.; Hull, P. J.; Hutchison, J. L. *Adv. Mater. (Weinheim, Germany)* **1994**, *6*, 772−775. Pehnt, M.; Schulz, D. L.; Curtis, C. J.; Jones, K. M.; Ginley, D. S. *Appl. Phys. Lett.* **1995**, *67*, 2176−2178. Schulz, D. L.; Pehnt, M.; Curtis, C. J.; Ginley, D. S. *Mater. Sci. Forum* **1996**, *225−227*, 169−174. Schulz, D. L.; Pehnt, M.; Rose, D. H.; Urgiles, E.; Cahill, A. F.; Niles, D. W.; Jones, K. M.; Ellingson, R. J.; Curtis, C. J.; Ginley, D. S. *Chem. Mater.* **1997**, *9*, 889−900. Schulz, D. L.; Curtis, C. J.; Flitton, R. A.; Wiesner, H.; Keane, J.; Matson, R. J.; Jones, K. M.; Parilla, P. A.; Noufi, R.; Ginley, D. S. *J. Electron. Mater.* **1998**, *27*, 433−437.

(6) Lau, M. L.; Strock, E.; Fabel, A.; Lavernia, C. J.; Lavernia, E. J. *Nanostruct. Mater.* **1998**, *10*, 723−730. Karthikeyan, J.; Berndt, C. C.; Tikkanen, J.; Reddy, S.; Herman, H. *Mater. Sci. Eng. A−Struct. Mater.* **1997**, *238*, 275−286.

(7) Goebbert, C.; Aegerter, M. A.; Burgard, D.; Nass, R.; Schmidt, H. In Beaucage, G., Mark, J. E., Burns, G. T., Hua, D. W., Eds.; Materials Research S: Warrendale, 1998; p 293−304. O'Hara, P. C.; Gelbart, W. M. *Langmuir* **1998**, *14*, 3418−3424. Ogawa, M.; Ishikawa, H.; Kikuchi, T. *J. Mater. Chem.* **1998**, *8*, 1783−1786.

(8) Decher, G.; Hong, J. D. *Ber. Bunsen-Ges. Phys. Chem. Chem.* **1991**, *95*, 1430.

(9) Decher, G. *Science* **1997**, *277*, 1232−1237.

10.1021/ja0029578 CCC: $20.00
Published on Web 01/17/2001

The LBL of nanoparticles can be described as the sequential adsorption of nanoparticles on oppositely charged layers of polyelectrolytes. The deposition of the films can be performed in a cyclic manner made possible by overcompensation of surface charge when polyelectrolytes or other species are adsorbed at the solid−liquid interface. The facile formation and stability of the nanoparticle LBL films should be attributed to the combination of both electrostatic and van der Waals attractive forces.[36,56] While the importance of the Coulomb interactions for LBL is rather obvious, the van der Waals intermolecular forces are considered to be weaker and are sometimes neglected. However, the LBL films made from uncharged compounds, whose formation was driven exclusively by the van der Waals interactions, have been recently reported.[37,81]

Being stimulated by the simplicity and universality of the assembly procedure, LBL films of nanoparticles are actively studied for a number of electronic and photonic applications.[11,19,20,31,38−55] At the same time, little is known about the fundamental regularities of this seemingly straightforward procedure. Only now are we beginning to understand how to manipulate different forces acting between polyelectrolytes and nanoparticles.[36,56,57] The importance of control over the film structure is difficult to overestimate for the functional optimization of numerous LBL-based materials and devices.

It is believed that each LBL adsorption step results in the formation of a continuous (mono)layer and the repetition of *n* deposition cycles yields a composite homogeneous film whose thickness is proportional to *n*. This is reflected as a linear increase of the mass or optical density, OD, of the LBL film with *n*. Here, we present the evidence that LBL growth can occur via two distinct modes. The buildup of LBL films of YIG and other nanoparticles can proceed as the enlargement of isolated 2D particle domains expanding laterally and vertically. Importantly, the dependence of the amount of YIG transferred to the substrate in each deposition cycle during lateral expansion still linearly depends on *n*, and therefore is undistinguishable from the true layer-by-layer growth when complete (mono)layers are formed in each adsorption step, i.e. the normal growth mode. The lateral expansion mode can occur for particles of different nature and, most likely, for many organic and inorganic

(10) Decher, G.; Hong, J. D. *Thin Solid Films* **1992**, *210/211*, 831. Decher, G.; Hong, J. D. *Ber. Bunsen-Ges. Phys. Chem. Chem.* **1991**, *95*, 1430. Stockton, W. B.; Rubner, M. F. *Macromolecules* **1997**, *30*, 2717−2725. Ferreira, M.; Cheung, J. H.; Rubner, M. F. *Thin Solid Films* **1994**, *244*, 806−809. Hsieh, M. C.; Farris, R. J.; McCarthy, T. J. *Macromolecules* **1997**, *30*, 8453−8458. Lvov, Y.; Onda, M.; Ariga, K.; Kunitake, T. *J. Biomater. Sci.−Polym. Ed.* **1998**, *9*, 345−355. Lvov, Y.; Decher, G.; Haas, H.; Möhwald, H.; Kalachev, A. *Phys. Status Solidi B* **1994**, *198*, 89−91. Balasubramanian, S.; Wang, X.; Wang, H. C.; Yang, K.; Kumar, J.; Tripathy, S. K. *Chem. Mater.* **1998**, *10*, 1554−1560. He, J. A.; Valluzzi, R.; Yang, K.; Dolukhanyan, T.; Sung, C.; Kumar, J.; Tripathy, S. K.; Samuelson, L.; Balogh, L.; Tomalia, D. A. *Chem. Mater.* **1999**, *11*, 3268−3274. He, J. A.; Bian, S.; Li, L.; Kumar, J.; Tripathy, S. K.; Samuelson, L. A. *Appl. Phys. Lett.* **2000**, *76*, 3233−3235.

(11) (a) Kotov, N. A.; Dekany, I.; Fendler, J. H. *J. Phys. Chem.* **1995**, *99*, 13065−13069. (b) Aliev, F.; Correa-Duarte, M.; Mamedov, A.; Ostrander, J. W.; Giersig, M.; Liz-Marzan, L.; Kotov, N. *Adv. Mater.* **1999**, *11*, 1006−1010.

(12) Ariga, K.; Lvov, Y.; Ichinose, I.; Kunitake, T. *Appl. Clay Sci.* **1999**, *15*, 137−152.

(13) Caruso, F.; Lichtenfeld, H.; Giersig, M.; Möhwald, H. *J. Am. Chem. Soc.* **1998**, *120*, 8523−8524.

(14) Caruso, F.; Caruso, R. A.; Möhwald, H. *Science (Washington, D.C.)* **1998**, *282*, 1111−1114.

(15) Correa-Duarte, M. A.; Giersig, M.; Kotov, N. A.; Liz-Marzan, L. M. *Langmuir* **1998**, *14*, 6430−6435.

(16) Koktysh D. S.; Kotov N. A.; Pastoriza-Santos I.; Liz-Marzan L. M.; Yun B.-G.; Matts R. L. *submitted to Coloids Surf.*

(17) Feldheim, D. L.; Grabar, K. C.; Natan, M. J.; Mallouk, T. E. *J. Am. Chem. Soc.* **1996**, *118*, 7640−7641.

(18) Gao, M. Y.; Richter, B.; Kirstein, S.; Möhwald, H. *J. Phys. Chem. B* **1998**, *102*, 4096−4103.

(19) Gao, M.; Kirstein, S.; Rogach, A. L.; Weller, H.; Möhwald, H. *Adv. Sci. Technol. (Faenza, Italy)* **1999**, *27*, 347−358.

(20) Kotov, N. A.; Magonov, S.; Tzopsha, E. *Chem. Mater.* **1998**, *10*, 886−895.

(21) Liu, Y.; Wang, Y.; Claus, R. O. *Chem. Phys. Lett.* **1998**, *298*, 315−319.

(22) Liu, Y.; Zhao, W.; Wang, Y. X.; Claus, R. O. *Proc. SPIE-Int. Soc. Opt. Eng.* **1998**, *3324*, 45−48.

(23) Lvov, Y.; Ariga, K.; Onda, M.; Ichinose, I.; Kunitake, T. *Langmuir* **1997**, *13*, 6195−6203.

(24) Lvov, Y. M.; Rusling, J. F.; Thomsen, D. L.; Papadimitrakopoulos, F.; Kawakami, T.; Kunitake, T. *Chem. Commun.* **1998**, 1229−1230.

(25) Lvov, Y.; Ariga, K.; Onda, M.; Ichinose, I.; Kunitake, T. *Langmuir* **1997**, *13*, 6195−6203.

(26) Mamedov, A.; Ostrander, J.; Aliev, F.; Kotov, N. A. *Langmuir* **2000**, *16*, 3941−3949.

(27) Pastoriza-Santos, I.; Koktysh, D. S.; Mamedov, A. A.; Giersig, M.; Kotov, N. A.; Liz-Marzan, L. M. *Langmuir* **2000**, *16*, 2731−2735.

(28) Ferguson, G. S.; Kleinfeld, E. R. *Adv. Mater.* **1995**, *7*, 414−416.

(29) Kleinfeld, E. R.; Ferguson, G. S. *Science* **1994**, *265*, 370−373.

(30) Bell, C. M.; Arendt, M. F.; Gomez, L.; Schmehl, R. H.; Mallouk, T. E. *J. Am. Chem. Soc.* **1994**, *116*, 8374−8375.

(31) Cassagneau, T.; Mallouk, T. E.; Fendler, J. H. *J. Am. Chem. Soc.* **1998**, *120*, 7848−7859.

(32) Keller, S. W.; Kim, H. N.; Mallouk, T. E. *J. Am. Chem. Soc.* **1994**, *116*, 8817−8818.

(33) Kovtyukhova, N. I.; Ollivier, P. J.; Martin, B. R.; Mallouk, T. E.; Chizhik, S. A.; Buzaneva, E. V.; Gorchinskiy, A. D. *Chem. Mater.* **1999**, *11*, 771−778.

(34) Mattoussi, H.; Radzilowski, L. H.; Dabbousi, B. O.; Fogg, D. E.; Schrock, R. R.; Thomas, E. L.; Rubner, M. F.; Bawendi, M. G. *J. Appl. Phys.* **1999**, *86*, 4390−4399.

(35) Schlenoff, J. B.; Ly, H.; Li, M. *J. Am. Chem. Soc.* **1998**, *120*, 7626−7634.

(36) Kotov, N. A. *Nanostruct. Mater.* **1999**, *12*, 789−796.

(37) Serizawa, T.; Hamada, K. I.; Kitayama, T.; Fujimoto, N.; Hatada, K.; Akashi, M. *J. Am. Chem. Soc.* **2000**, *122*, 1891−1899.

(38) Keller, S. W.; Johnson, S. A.; Brigham, E. S.; Yonemoto, E. H.; Mallouk, T. E. *J. Am. Chem. Soc.* **1995**, *117*, 12879−12880.

(39) Kerimo, J.; Adams, D. M.; Barbara, P. F.; Kaschak, D. M.; Mallouk, T. E. *J. Phys. Chem. B* **1998**, *102*, 9451−9460.

(40) Baur, J. W.; Kim, S.; Balanda, P. B.; Reynolds, J. R.; Rubner, M. F. *Adv. Mater.* **1998**, *10*, 1452−1455.

(41) Baur, J. W.; Rubner, M. F.; Reynolds, J. R.; Kim, S. *Langmuir* **1999**, *15*, 6460−6469.

(42) Cheung, J. H.; Fou, A. F.; Rubner, M. F. *Thin Solid Films* **1994**, *244*, 985−989.

(43) Mattoussi, H.; Radzilowski, L. H.; Dabbousi, B. O.; Thomas, E. L.; Bawendi, M. G.; Rubner, M. F. *J. Appl. Phys.* **1998**, *83*, 7965−7974.

(44) Rubner, M. F. *J. Macromol. Sci. Pure Appl. Chem.* **1994**, *A31*, 805−809.

(45) Lenahan, K. M.; Wang, Y. X.; Liu, Y.; Claus, R. O.; Heflin, J. R.; Marciu, D.; Figura, C. *Adv. Mater.* **1998**, *10*, 853−855.

(46) Liu, Y. J.; Wang, A. B.; Claus, R. *J. Phys. Chem. B* **1997**, *101*, 1385−1388.

(47) Liu, Y. J.; Wang, A. B.; Claus, R. O.; Jiang, E. Molecular Self-Assembly of Fe_3O_4/Polyimide Nanocomposite Films (I). In *Magnetic Ultrathin Films, Multilayers*; Tobin, J., Chambliss, D., Kubinski, D., Barmak, K., Dederichs, P., Dejonge, W., Katayama, T., Schuhl, A., Eds.; Materials Research S: Warrendale, 1997; pp 39−47.

(48) Kotov, N. A.; Dekany, I.; Fendler, J. H. *Adv. Mater.* **1996**, *8*, 637.

(49) Rogach, A. L.; Koktysh, D. S.; Harrison, M.; Kotov, N. A. *Chem. Mater.* **2000**, *12*, 1526−1528.

(50) Caruso, F.; Donath, E.; Möhwald, H.; Georgieva, R. *Macromolecules* **1998**, *31*, 7365−7377.

(51) Möhwald, H.; Lichtenfeld, H.; Moya, S.; Voigt, A.; Baumler, H.; Sukhorukov, G.; Caruso, F.; Donath, E. *Macromol. Symp.* **1999**, *145*, 75−81.

(52) Gao, M.; Lesser, C.; Kirstein, S.; Möhwald, H.; Rogach, A. L.; Weller, H. *J. Appl. Phys.* **2000**, *87*, 2297−2302.

(53) Hong, H.; Davidov, D.; Chayet, H.; Faraggi, E. Z.; Tarabia, M.; Avny, Y.; Neumann, R.; Kirstein, S. *Supramol. Sci.* **1997**, *4*, 67−73.

(54) Hong, H.; Davidov, D.; Tarabia, M.; Chayet, H.; Benjamin, I.; Faraggi, E. Z.; Avny, Y.; Neumann, R. *Synth. Met.* **1997**, *85*, 1265−1266.

(55) He, J. A.; Yang, K.; Kumar, J.; Tripathy, S. K.; Samuelson, L. A.; Oshikiri, T.; Katagi, H.; Kasai, H.; Okada, S.; Oikawa, H.; Nakanashi, H. *J. Phys. Chem. B* **1999**, *103*, 11050−11056.

(56) Dubas, S. T.; Schlenoff, J. B. *Nacromolecules* **1999**, *32*, 8153−8160.

(57) Hammond, P. T. *Curr. Opin. Colloid Interface Sci.* **2000**, *4* (6), 430.

colloids as demonstrated here with barium ferrite and latex dispersions. Different compensation mechanisms are suggested to contribute to the linearity of the lateral expansion mode.

The possibility of the lateral mode of film buildup must be taken into account when designing complex multilayer systems. The order in the stack of the layers with different functionalities will be disrupted by the irregular nature of the particle domains. Therefore, we also discuss here the approaches to switching from the lateral expansion mode to the normal growth mode when each deposition cycle results in the addition of a complete layer perpendicular to the normal to the surface. In particular, this can be achieved by grafting organic moieties to the surface of nanoparticles. The hydrocarbon groups enhance the van der Waals component of the attractive force between nanoparticles and polyelectrolytes. Consequently, the nanoparticles adsorbed in each deposition step produce a densely packed layer, and the layer-by-layer deposition resulting in uniform multilayer assemblies is realized.

Experimental Section

1. Preparation of the YIG Colloid. Nanopowders of YIG and barium ferrite were purchased from the Nanomaterials Research Corporation (Logmont, CO). According to the company specifications, the average diameter of particles was 50 nm as determined by BET (company's specifications). Approximately 0.5 g of the nanopowder was initially suspended in 250 mL of 18.2 MΩ deionized water (Barnstead, E-pure system) with the pH adjusted to 11.23 with NH_4-OH (Aldrich). The dispersion was ultrasonically agitated in a Whatman Sonicor SC-50T ultrasound bath for not less than 2 h and the resulting suspension was allowed to stand for at least 1 h. The heaviest particles were sedimented by centrifugation at 3800 rpm for 10 min in Centrific centrifuge (Fisher), and the supernatant containing dispersed YIG particles was decanted and stored for subsequent use in the LBL deposition. Suspended particles had an average particle size of 30 nm as determined by transmission electron microscopy (TEM). The suspensions of barium ferrite were prepared according to the identical procedure.

2. Modification of YIG Colloid. About 2 g of YIG powder was thoroughly dried in a vacuum for 1 day to remove traces of water. Then, the sample was transferred into a 50 mL hexane 0.5% solution of 3-aminopropyl trimethoxysilane (Fluka) and the mixture was stirred in an airtight flask for 24 h. After that, the solid was decanted and washed with a large amount of dry hexane, acetone, and finally ethanol. The modified nanoparticles were dispersed in water at acidic pH <4 in an analogous way to the nonmodified nanoparticles. The dispersions of equal optical density were used in the layer-by-layer assembly procedure in each case.

3. Layer-by-Layer Assembly. Glass slides and silicon wafers used as film substrates were cleaned with Nochromix (Fisher) in concentrated H_2SO_4, then thoroughly rinsed and allowed to dry in air. An appropriate substrate was immersed in a 1% aqueous solution of high molecular weight poly(diallyldimethylammonium chloride), Mw = 400000−500000 (Aldrich), for 10 min at pH 3.5 and rinsed with deionized 18 MΩ water in three beakers for 1 min each. To remove the excess liquids from the substrate surface, the samples were dried in a stream of compressed air. After that, the slide was immersed into a beaker containing the YIG suspension for 1 h. Upon completion of the nanoparticle adsorption, the substrate was removed, rinsed in two beakers of fresh 18 MΩ water for 1 min each, and then dried. To form multilayers, the entire cycle of PDDA and YIG adsorption was repeated as many times as necessary to obtain a film of the desired thickness.

Two modifications of the basic LBL procedure described above were used in this study: (1) YIG was assembled in the presence of NaCl followed the procedure outlined above with the exception that the stock 20% solution of PDDA was diluted with a solution of NaCl of required concentration in the amount necessary to obtain a 1% PDDA solution. (2) The LBL assembly of YIG nanoparticles was also performed after the deposition of several polyelectrolyte/polyelectrolyte LBL layers (precursor layers). The first layer of PDDA was prepared as described above at pH 3.5. After that, a layer of poly(acrylic acid) [PAA, Mw = 1000000] or (polystyrenesulfonate sodium) [PSS, Mw =1000000] was deposited by immersion of a substrate in 1.0% aqueous solution of the polyelectrolyte at pH 3.5 for 10 min. The substrates were then rinsed three times for 1 min in three separate beakers. For preparation of precursor layers, the polyelectrolyte assembly was repeated until five (PDDA/PAA) layers topped with a layer of PDDA were made. After that, the substrate was exposed to the YIG dispersion and YIG/PDDA alternations continued as usual.

4. Instrumentation. The progress of the nanoparticle assembly on glass substrates was monitored by using UV−vis spectra on an HP8453A Hewlett-Packard spectrophotometer. The UV−vis readings were taken after each assembled layer. The dependence of the adsorption increment on the number of layers was observed at 350 nm.

YIG films assembled on silicon wafers were analyzed by atomic force microscopy (AFM). AFM images were taken by using a Multimode Nanoscope IIIa instrument operating in the tapping mode with TESP silicon nitride tips. Typically, the surface was scanned at 2 Hz with 256 lines per image resolution and 1.2−4.0 V set-point.

Transmission electron microscopy (TEM) images were taken on a JEOL JEM 100 CX II scanning transmission electron microscope with a Noran X-ray system operating at 100 kV. TEM samples were prepared so that a layer of magnetic nanoparticles was deposited only on one side of the carbon-coated TEM grid. A 200 mesh copper grid was carefully brought into contact with the surface of aqueous solutions and was allowed to float on the air−water interface for the period of time equivalent to the duration of adsorption in a regular deposition cycle. Then, the grid was cautiously removed from the solution avoiding the contact of its backside with the subphase and was transferred onto the surface of the next solution.

Scanning electron microscopy (SEM) images were taken on a JEOL JXM 6400 scanning electron microscope with an Oxford exL X-ray system and cryostage operating at an accelerating voltage of 15−20 kV and a field depth of 8. The samples were coated with gold in a Denton Vacuum Desk II magnetron sputterer/etcher.

Ellipsometric measurements were made with an AutoEL MS ellipsometer from Rudolph Research Corp. The measurements are performed with use of a 632.8 nm line of He/Ne laser incident upon the sample at 70°. The so-called DafIBM program supplied by Rudolph Technologies is employed to determine the thickness values.

The ζ-potential measurements were performed by using Malvern Zetasizer 2000 HS operating with the internal 10 mW, 633 nm He−Ne laser in the right angle geometry. The standard 1 × 1 cm cuvette was used in these measurements. ζ-potentials of PDDA, PAA, and PSS layers were determined by adsorbing the polyelectrolytes on 200 nm latex particles.[58] The latex dispersion was added to the corresponding polyelectrolyte with pH adjusted to the required value and remained there for 30 min. After gentle centrifugation and rinsing with water, the particles were redispersed in water with appropriate pH and the ζ-potential of latex particles was measured in the regular fashion.

Results and Discussion

1. YIG Particles. The starting point of the LBL deposition of nanoparticles is the preparation of an aqueous dispersion of the inorganic material. The surface potential of a colloid should be high enough to overcome attractive forces between the particles that can be balanced by the electrostatic repulsion of double electrical layers. For YIG, the isoelectric point is located at pH 6−7,[59] and therefore, both basic and acidic pH should result in charging of the YIG surface. The most stable dispersions of YIG were obtained at pH 11.23, where YIG particles are negatively charged. They were stable for months

(58) Caruso, F.; Donath, E.; Möhwald, H. *J. Phys. Chem. B* **1998**, *102*, 2011−2016.

(59) Kuroda, Y.; Hamano, H.; Mori, T.; Yoshikawa, Y.; Nagao, M. *Langmuir*. In press. Tombacz, E.; Dobos, A.; Szekeres, M.; Narres, H. D.; Klumpp, E.; Dekany, I. *Colloid Polym. Sci.* **2000**, *278*, 337−345. Preocanin, T.; Brzovic, Z.; Dodlek, D.; Kallay, N. *Prog. Colloid Polym. Sci.* **1834**, *112*, 76−79. Shen, J.; Ebner, A. D.; Ritter, J. A. *J. Colloid Interface Sci.* **1999**, *214*, 333−343.

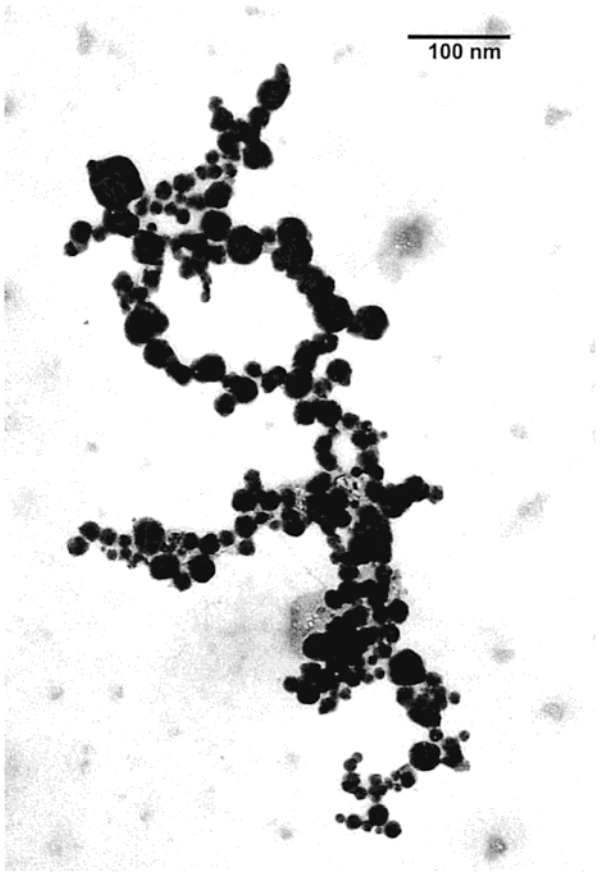

Figure 1. Transmission electron microscopy image of YIG nanoparticles in aqueous dispersion used for LBL assembly.

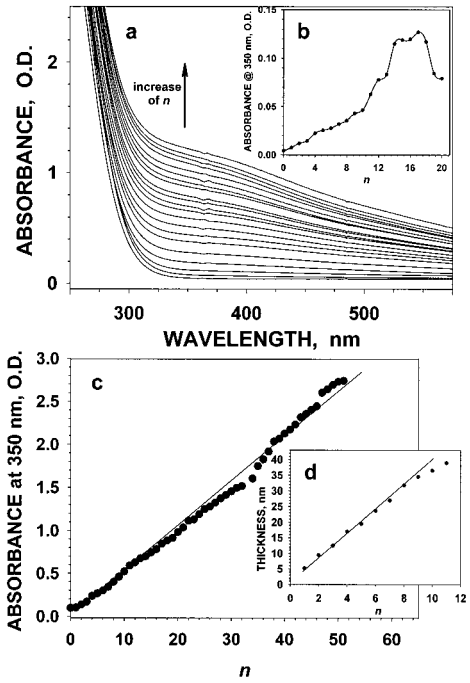

Figure 2. (a) UV−vis absorption spectra of $(PDDA/YIG)_n$, $n = 1-20$, films sequentially adsorbed on a glass slide. (b) Dependence of the optical density of the $(PDDA/YIG)_n$ film with 20 min of the YIG absorption step. (c) Dependence of the optical density of $(PDDA/YIG)_n$, $n = 1-50$, films at 350 nm assembled with 1 h of the YIG adsorption step. (d) Ellipsometric thickness of $(PDDA/YIG)_n$, $n = 1-10$, sequentially deposited on a glass slide and registered at 632.8 nm. The thickness increment per YIG layer is 3.5 nm, the precursor layer thicknessis 4 nm, $n_{YIG} = 1.9$, and $n_{precursor} = 1.7$.

without any sign of precipitation. In comparison with silica or titania of similar particle size forming stable dispersions in mildly basic or acidic solutions, pH of the YIG dispersions is somewhat higher, which is likely to be related to additional, relatively weak magnetic forces between them. As evidenced by the transmission electron microscopy, prepared dispersions are fairly polydispersed with particles ranging from 15 to 50 nm in diameter (Figure 1). The average diameter of the particles was 32 nm. Addition of 0.1% PDDA resulted in formation of a red sediment, which cannot be further redispersed.

2. Layer-by-Layer Assembly of YIG. Layer-by-layer assembly is based on a cyclic adsorption of positively and negatively charged species, say **A** and **B**, by dipping a substrate alternatively into their solutions, which results in a layered blend of **A** and **B**. The only requirement to **A** and **B** is to be of relatively high molecular weight, which makes LBL a very versatile deposition technique. Heavy mass and multiple points of attachment to **A** and **B** render the absorption sufficiently irreversible to allow for the deposition of the next layer. Either **A** or **B** is almost always a polyelectrolyte,[9] while the other LBL partner can be a dispersion of nanoparticles, clay sheets, proteins, dyes, vesicles, DNA, viruses, or other species. The omnipresence of polyelectrolytes in the LBL assemblies is explained by their ability to cover irregularities in the surface they adsorb on owing to rodlike conformation of the charged macromolecules in aqueous solutions.[9,60] It is commonly understood that both **A** and **B** form a complete (mono)layer on the surface, which is dense enough to reverse the surface charge in each layer. Indeed, for many combinations of oppositely charged compounds each adsorption step produces a thin and uniform layer of a corresponding compound. However, for many combinations of polyelectrolytes with compact colloidal species (organic or inorganic), the growth of the LBL assembly was shown to be very slow or irregular for reasons which remain poorly understood and which we hoped to clarify in this work.

An LBL film obtained after n deposition cycles can be generically referred to as $(\mathbf{A}/\mathbf{B})_n$, and this notation will be used throughout the paper. It is important to note that the $(\mathbf{A}/\mathbf{B})_n$ abbreviation describes primarily the *deposition procedure* rather than the actual sequence of the multilayers obtained as a result of it. The films, where the adjacent layers deposited in one cycle can be clearly distinguished from each other, are difficult to obtain because of the strong interpenetration of polyelectrolyte chains[61−63] blurring the border between the adjacent layers although some advances in this direction have been recently made.[26,64]

The layer-by-layer deposition of YIG nanoparticles on glass substrate was monitored by the increase of the UV−vis absorbance, OD, when particles were deposited on a transparent substrate (Figure 2). The stable growth of the LBL assembly, resulting in the repeatable deposition of layers of polyelectrolyte and nanoparticles, must yield a linear dependence of OD vs the number of layers, n, as was reported for many LBL assembly pairs.[11−31,65,66] Interestingly, both smooth saturated log-like dependencies and curves with multiple inflection points were observed for YIG nanoparticles in some experiments (Figure

(60) Kotov, N. A.; Haraszti, T.; Turi, L.; Zavala, G.; Geer, R. E.; Dekany, I.; Fendler, J. H. *J. Am. Chem. Soc.* **1997**, *119*, 6821−6832.

(61) Decher, G.; Lvov, Y.; Schmitt, J. *Thin. Solid. Films* **1994**, *244*, 772−777.

(62) Lvov, Y.; Decher, G.; Möhwald, H. *Langmuir* **1993**, *9*, 481−486.

(63) Lvov, Y.; Decher, G.; Haas, H.; Möhwald, H.; Kalachev, A. *Phys. Status Solidi B* **1994**, *198*, 89−91.

(64) Tarabia, M.; Hong, H.; Davidov, D.; Kirstein, S.; Steitz, R.; Neumann, R.; Avny, Y. *J. Appl. Phys.* **1998**, *83*, 725−732.

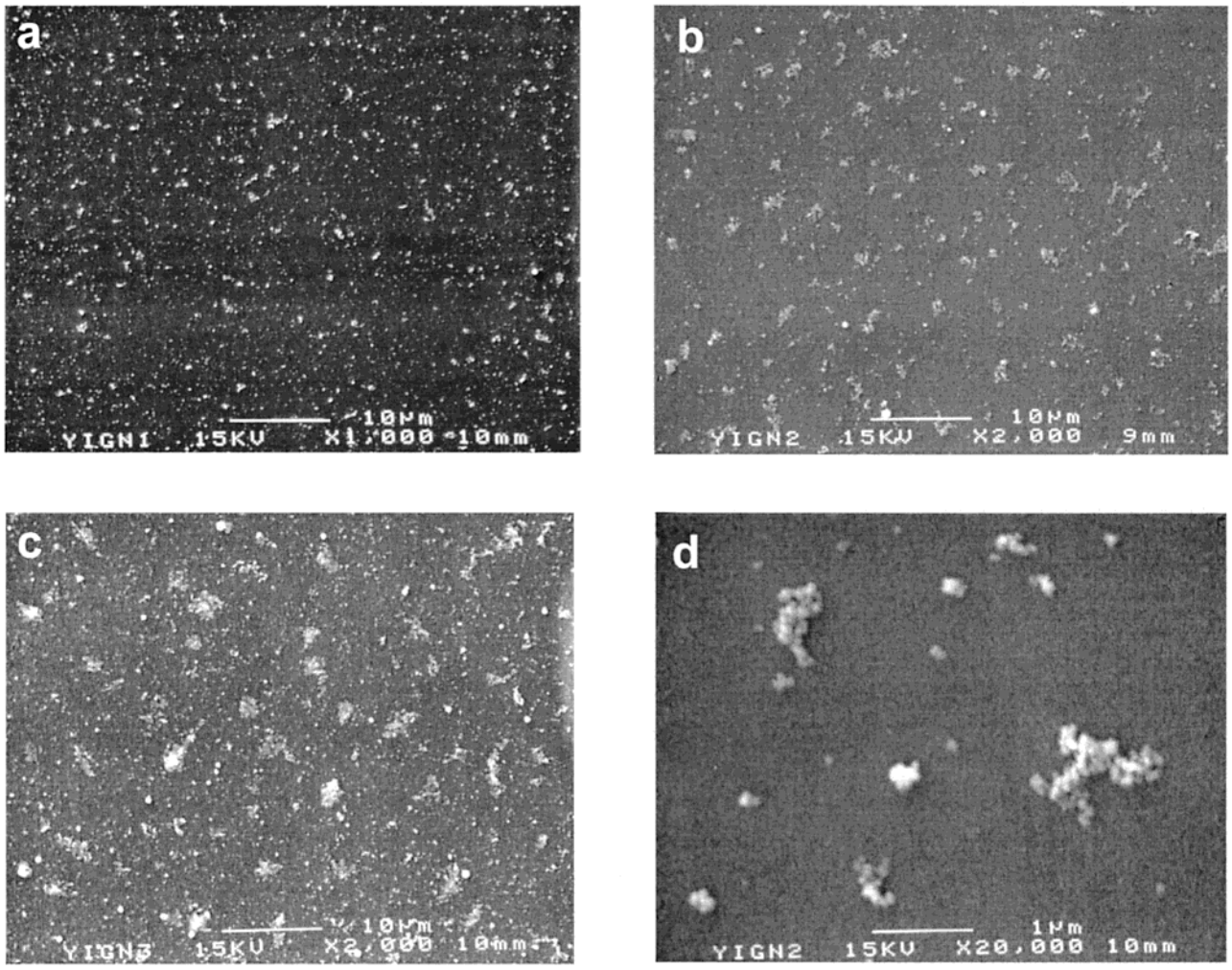

Figure 3. Scanning electron microscopy images of $(PDDA/YIG)_n$ films with (a) $n = 1$, (b and d) 2, and (c) 3.

2b). The stable linear growth was obtained when the time of exposure of the substrate to the YIG dispersion was increased from a few minutes to 1 h (Figure 2c). Elongation of the exposure time for YIG to 12 h did not significantly affect OD vs *n* dependence.

Measurements of the thickness of the LBL films by ellipsometry (Figure 2d) reveal that the average film thickness linearly increases with the number of deposition cycles in line with the dependence of OD. The thickness increment, which is being added to the coating by a single PDDA/YIG layer, is 3.5 nm. If we recall the fact that the average diameter of YIG nanoparticles is 32 nm, then this thickness corresponds to the average surface density of YIG of one particle per 32300 nm^2. Such a small thickness of absorption layer and a low density of particles contradict the structure of LBL nanoparticle films found in previously studied LBL pairs.[11,21,23,24,26,27,49,65−69] Considering the requirement of the surface charge switching,[35] the sustained buildup of the multilayers seen in Figures 2b and 3 becomes quite surprising and raises the question about the actual mechanism of the layer-by-layer growth in this case. Note that the stable growth of YIG/PDDA multilayers is observed for as long as 50 deposition cycles. The number of layers is large enough to defy any doubts that it will continue further in the same fashion.

Scanning electron microscopy investigation of the surface topography enabled us to resolve this contradiction. The SEM images revealed that the repetition of adsorption cycles resulted not in the sandwich-like layering of organic and inorganic strata, as was observed or assumed to be present for numerous other LBL pairs,[11,21,23,24,26,27,49,65−69] but rather in the growth of fairly isolated YIG islands (Figure 3). In layer 1, the film consists of YIG domains 0.5−1.5 μm in diameter (Figure 3a), which increase to 1−3 μm in deposition cycle 2 (Figure 3b), and 3−4 μm in deposition cycle 3 (Figure 3c). The domains are laterally expanding along the substrate surface, which is also accompanied by the increase of their average height. In the closeup, one can see that the YIG islands are 3D agglomerates of YIG nanoparticles (Figure 3d), growing in size with increasing *n*. The AFM examination of the same film showed that the surface of the substrate between the YIG domains is coated only by the polyelectrolyte (Supporting Information). The topography in the gaps is virtually featureless with very small roughness, which is characteristic of PDDA. This demonstrates that the particles deposited in the LBL deposition cycles adhere predominantly to the existing domains rather than to the bare PDDA-covered surface, although the total number of domains may also increase.

The growth pattern of the isolated YIG domains, which for convenience will be referred to here as the lateral expansion

(65) Schrof, W.; Rozouvan, S.; Vankeuren, E.; Horn, D.; Schmitt, J.; Decher, G. *Adv. Mater.* **1998**, *10*, 338−341.
(66) Gao, M.; Zhang, X.; Yang, B.; Li, F.; Shen, J. *Thin Solid Films* **1996**, *284−285*, 242−245.
(67) Mamedov, A. A.; Kotov, N. A. *Langmuir* **2000**, *16*, 5530−5533.
(68) Rosidian, A.; Liu, Y. J.; Claus, R. O. *Adv. Mater.* **1998**, *10*, 1087.
(69) Liu, Y.; Wang, A.; Claus, R. O. *Appl. Phys. Lett.* **1997**, *71*, 2265−2267.

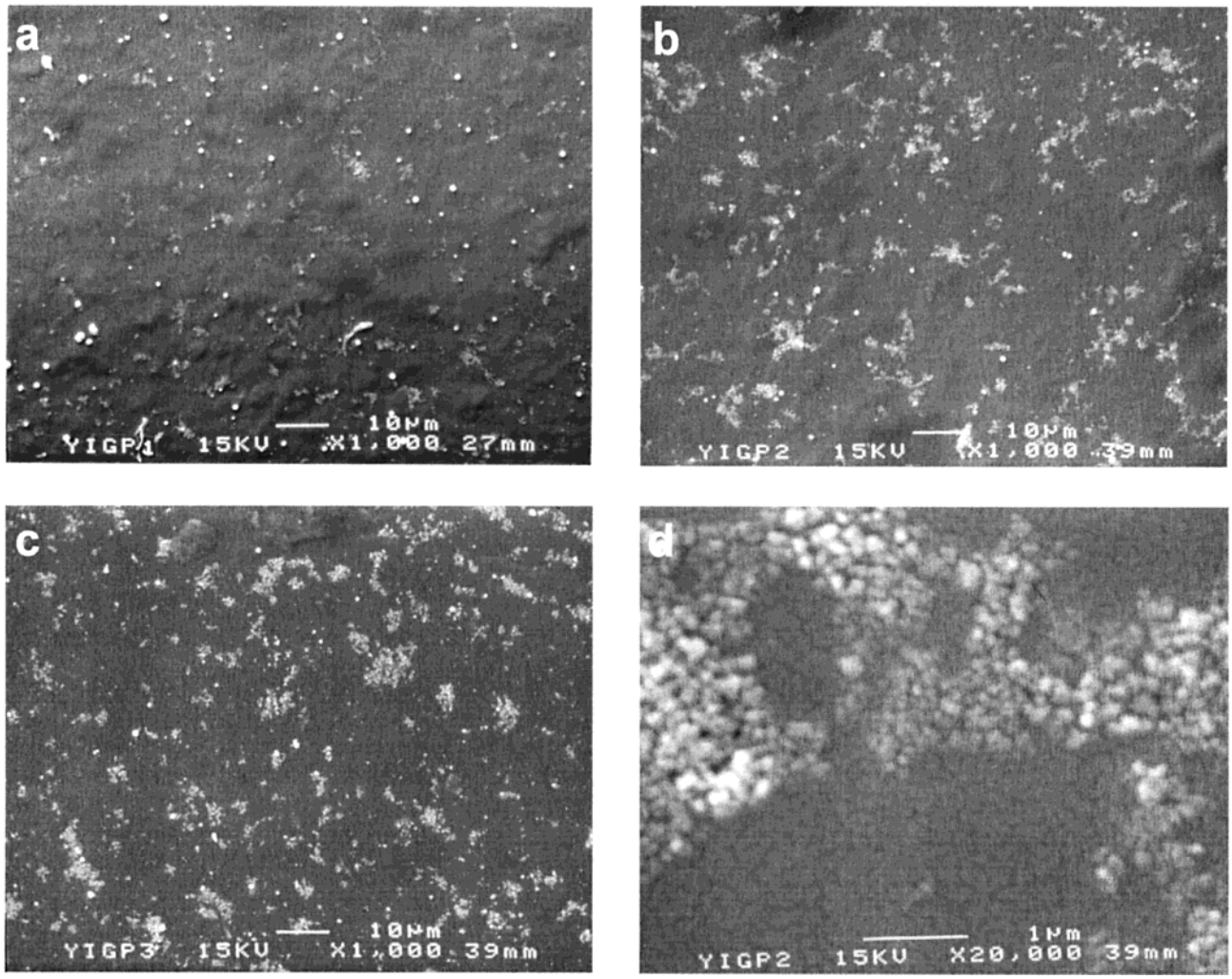

Figure 4. Scanning electron microscopy images of $(PDDA/YIG)_n$ films with (a) $n = 1$, (b and d) 2, and (c) 3 assembled on a precursor layer $(PDDA/PAA)_5PDDA$.

mode,[70] was initially regarded as the result of poor quality substrate carrying probably hydrophobic patches as was seen for modified silica surfaces.[71] However, for glass slides and silicon wafers thoroughly cleaned with hot piranha solution for as long as 30 min as well as for glass slides treated with a promoter of polyelectrolyte adsorption 3-aminopropylsiloxane, the identical deposition patterns were observed. Effective elimination of a potential substrate effect can be accomplished by precoating it with a $(PDDA/PAA)_n$ multilayer to form a precursor film, which makes the surface virtually uniform in properties. $(PDDA/PAA)_n$ and similar polyelectrolyte pairs were shown by many authors to form excellent coatings on a variety of surfaces.[72−77] We used acidic pH 3.5 for PAA solution, when PAA is only slightly ionized, to increase the thickness of the adsorption layers.[73] Five (PDDA/PAA) bilayers were made on a substrate producing a film of ca. 20 nm and topped with an additional layer of PDDA. This rendered the substrate hydrophilic with a contact angle of $37 \pm 3°$. Regardless of the very hydrophilic nature of the $(PDDA/PAA)_nPDDA$ film, a new series of SEM images reveals that the cyclic repetition of adsorption steps results in the same growth pattern as for the bare silicon wafers without the precursor film (Figure 4). The size of the YIG domains expands from 1.5 to 2 μm for the first dipping cycle (Figure 4a) to 3−5 μm for cycle 2 (Figure 4b) and 5−7 μm for cycle 3 (Figure 4c). Between the YIG islands, one can see the texture of the underlying precursor layer both on the low magnification and high magnification images (Figure 4d with Figure 3d); surface relief of the precursor layer is different from the corresponding background textures in Figure 3.

Thus, one can conclude that the pattern of film growth seen in Figures 3−5 is a feature of the particle/polyelectrolyte pair rather than the substrate effect. Since the forces between YIG and PDDA are of rather general nature, i.e. not specific to the YIG−polyelectrolyte pair, a similar growth pattern is likely to occur in other systems involving nanoparticles or other colloids. Indeed, the similar lateral domain expansion can be seen for 40 nm barium ferrite nanoparticles and 200 nm polystyrene latex (Figure 5).

Considering the structure of the films in Figures 3−5, it must be pointed out that there is an aspect of the deposition process that is quite difficult to rationalize at the moment. The constantly

(70) This term is used with the understanding that concomitant with the lateral expansion, the domains also grow in thickness accumulating new layers of particles similarly to the normal growth mode.

(71) Ferguson, G.; Kleinfeld, E. *Chem. Mater.* **1996**, *8*, 1575−1578.
(72) Joly, S.; Kane, R.; Radzilowski, L.; Wang, T.; Wu, A.; Cohen, R. E.; Thomas, E. L.; Rubner, M. F. *Langmuir* **2000**, *16*, 1354−1359.
(73) Shiratori, S. S.; Rubner, M. F. *Macromolecules* **2000**, *33*, 4213−4219.
(74) Mendelsohn, J. D.; Barrett, C. J.; Chan, V. V.; Pal, A. J.; Mayes, A. M.; Rubner, M. F. *Langmuir* **2000**, *16*, 5017−5023.
(75) Caruso, F.; Furlong, D. N.; Ariga, K.; Ichinose, I.; Kunitake, T. *Langmuir* **1998**, *14*, 4559−4565.
(76) Chen, W.; McCarthy, T. J. *Macromolecules* **1997**, *30*, 78−86.
(77) Lvov, Y.; Ariga, K.; Ichinose, I.; Kunitake, T. *Langmuir* **1996**, *12*, 3038−3044.

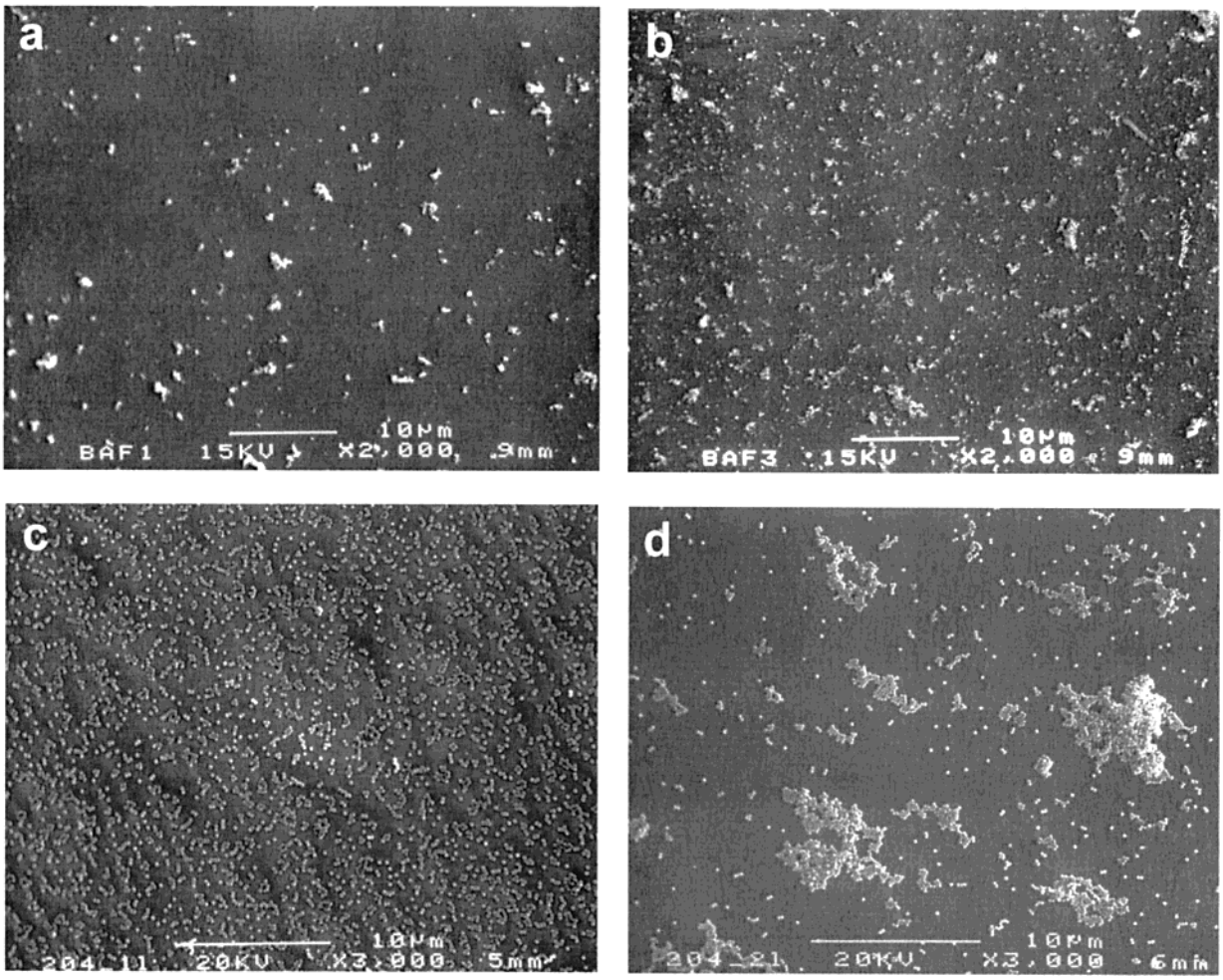

Figure 5. Scanning electron microscopy images of (PDDA/barium ferrite)$_n$ films with (a) $n = 1$ and (b) 2 and (PDDA/latex)$_n$ films with (c) $n = 1$ and (d) 2.

expanding area of YIG islands is supposed to increase the amount of material transferred in each deposition cycle, and therefore should result in a constantly increasing optical density increment. For all these cases, particularly surprising is the fact that the OD vs n plot remains linear throughout the deposition process without any sign of upturn. This indicates that there is a compensation effect reducing the number of adsorbed particles as the area of the film expands. There can be several possible mechanisms of the compensation: (1) partial desorption of previously adsorbed particles during the adsorption of the next polyelectrolyte layer; (2) increased electrostatic repulsion between like charged components as the film grows; and (3) dependence of the amount of the adsorbed material on film/substrate roughness.

The presence of the nanoparticle desorption process associated with the deposition of the new PDDA layers can be clearly seen in Figure 2b: the reduction of the YIG UV absorbance with increasing n can only be explained by partial removal of YIG particles.[78] The reduction of the number of free-standing latex spheres after the second deposition cycle can also be clearly seen in Figure 6d. The increase of electrostatic repulsion and the influence of roughness on the amount of adsorbed material can be predicted on the basis of refs 79. Hence, the compensationmechanisms are to be present in the system. Nevertheless, the question why the superposition of all these effects results in a linear growth and not in a higher order curve remains open. Further discussion of these processes and their relation to LBL deposition involves special theoretical treatment of the polyelectrolyte−nanoparticle−substrate system and goes beyond the scope of this publication.

3. Switching the Growth Modes. For the preparation of various thin film materials and devices from LBL assemblies of nanoparticles, it is always desirable to have a complete, densely packed adsorption layer rather than particle domains because the multilayers growing laterally do not allow for the control of the layer-by-layer architecture. Therefore, one needs to have some means to switch the modes of the LBL growth. The particle density in the absorption layer can possibly be increased by screening the electrostatic repulsion between the nanoparticles, i.e. by elevating the ionic strength, I, of dispersion, which was shown to increase the thickness of the LBL layers of polyelectrolytes.[61,73] Indeed, with addition of NaCl to YIG, the slope of the OD vs n plot becomes steeper than that for pure YIG (Figure 6a). The dependence of $\partial OD/\partial n$ vs I shows a significant increase of the number of particles transferred in each cycle for [NaCl] < 0.2 M. $\partial OD/\partial n$ passes through the maximum at ca. 0.2 M NaCl, leveling off at 0.5 M NaCl (Figure 6b).[80] The structure of the film in a maximum of $\partial OD/\partial n$ at

(78) The substrates with YIG/PDDA films were air-dried between the deposition cycles. The accelerated drying in the stream of gas was intentionally avoided.

(79) Hartley, P. G.; Scales, P. J. *Langmuir* **1998**, *14*, 6948−6955. Hoogeveen, N.; Cohen Stuart, M. A.; Fleer, G. J. *J. Colloid Interface Sci.* **1996**, *182*, 146−157. Sukhishvili, S.; Granick, S. *J. Chem. Phys.* **1998**, *109*, 6869−6878. Sukhishvili, S.; Granick, S. *J. Chem. Phys.* **1998**, *109*, 6861−6868. Wallin, T.; Linse, P. *J. Chem. Phys.* **1998**, *109*, 5089−5100.

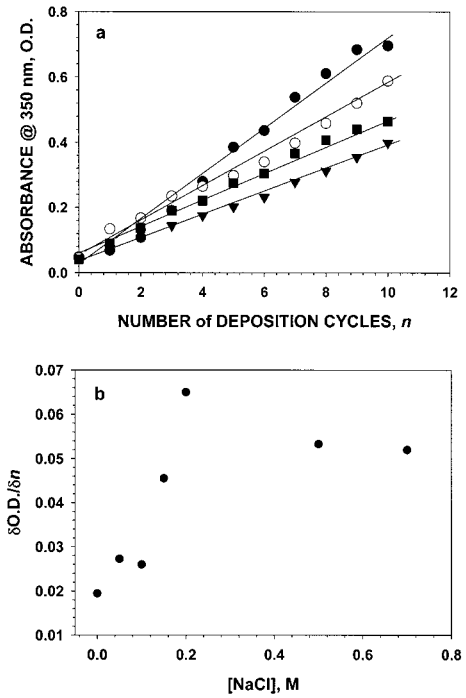

Figure 6. (a) Dependence of optical density at 350 nm for assembly of YIG from the solution of NaCl with a concentration of 0.0 (▼), 0.15 (■), 0.2 (●), and 0.5 M (○). The film was deposited only on one side of the glass slide. (b) Dependence of the slope of the linear plots in part a on the NaCl concentration.

[NaCl] = 0.2 M was investigated by SEM (Figure 7). The images reveal film morphology analogous to that observed in Figures 3−5, and hence the increase of ionic strength does not change the growth mode.

The addition of NaCl reduces the repulsion between the nanoparticles, but it also reduces the attraction between YIG and PDDA. Therefore, the increase in ionic strength results in both positive and negative effects in respect to increasing the surface density of nanoparticles. A different type of forces between nanoparticles and PDDA that ought to affect the film structure are the van der Waals interactions.[36] So far, these forces were paid little attention in the studies of the layer-by-layer assembled films[36,56,57] although they are known to make the major contribution in the strength of polyelectrolyte complexes.[36,56,82] In particular, we want to utilize the hydrophobic interactions, which represent a special type of van der Waals forces with large entropic contribution.[83] They emerge in aqueous environments between fairly hydrophobic groups and can make a significant contribution to the overall energy balance as much as −7.5 kJ/mol per $-CH_2-$ group.[83] Moreover, the amplification of hydrophobic interactions will increase the attraction of the nanoparticles *both* to polyelectrolyte *and* to each other unlike the increase of ionic strength.

The surface of YIG is very hydrophilic. To retain the dispersability of nanoparticles in water and impart the ability to hydrophobically interact with the polyelectrolyte, one needs to modify their surface with a charged organic group. The hydrocarbon chain will result in efficient attraction to similar organic groups in the polyelectrolyte, while the surface charge will prevent irreversible coagulation of the nanoparticle colloid. This was accomplished by grafting a short 3-aminopropyl hydrocarbon chain through a siloxane bridge to the nanoparticle surface as described in the Experimental Section.

Since the modified YIG nanoparticles are positively charged, their thin film assembly was performed with negatively charged polyelectrolytes such as poly(styrenesulfonate), PSS, and PAA. For both polymers, the $\partial OD/\partial n$ is significantly greater than that for nonmodified YIG. In particular, for assembly with 0.5% PAA at pH 3.5 and assembly time 1 h, the $\partial OD/\partial n$ increases 5 times in comparison with naked YIG (Figure 8). SEM also reveals great improvement of the film structure: the nanoparticles are densely packed after only one deposition cycle (Figure 9a). The size of the aggregates visible in the image is much smaller than that for nonmodified YIG and does not exceed 0.5 μm in diameter. As the number of deposition cycles increases, the topography of the film shows little change with the exception of greater density of the particles and their aggregates (Figure 9b).

When YIG is modified with 3-aminopropyl siloxane both electrostatic and van der Waals components of particle−polyelectrolyte interactions are changed. However, the difference of the behavior of the modified YIG cannot be attributed to the difference in the electrostatic *attraction* between the nanoparticles and corresponding polyelectrolytes. The ζ-potentials[84] of the modified YIG and PSS at pH 3.5 are +12 and +15 mV, while ζ-potentials of the naked YIG and PDDA at pH 11 are −17 and −12 mV. As one can see, the magnitudes of the potentials are virtually the same for both LBL pairs, and therefore the long-distance Coulomb interaction between the nanoparticles and the polyelectrolyte-coated substrate is nearly the same for both pairs. To this point, it is necessary to add that the initial approach of both naked and modified particles at their corresponding pH to the polyelectrolyte covered surfaces causes electrostatic *repulsion* between the particle and the substrate because the ζ-potentials are of the same sign for each pair under the assembly conditions. Apparently, this does not forbid the layer-by-layer process because the polyelectrolytes at the physical border between the PDDA or PSS and water remain largely ionized, whereas the ζ-potential reflects the integral potential from the Stern layer and a part of the diffuse layer. The electrostatic repulsion of the outer layers of the ionic atmospheres creates the energetic barrier for adsorption, which is overcome due to the kinetic energy of the heavy nanoparticles followed by the engagement of short-range attractive interactions.

Thus, the increase in surface density of nanoparticles for modified YIG we primarily attributed to the attractive interactions between hydrocarbon groups or organic modifier and the polyelectrolyte chains adsorbed to the substrate. We also considered that some contribution could also be made by

(80) The addition of low molecular weight salt reduces the strength of both electrostatic repulsion between the particles and the electrostatic attraction between the polyelectrolyte and the colloid. Several other Coulomb pairs in the polyelectrolyte−nanoparticle−substrate system (inclusive counterions) are also affected. Therefore, high ionic strength can decrease or increase the surface density of nanoparticles in the adsorption layer. Besides that, there are also other factors affected by the ionic strength such as the size of dynamic agglomerates of YIG and collapse of the polyelectrolyte brush at the substrate−water interface. All these effects yield the complex nonmonotonic dependence of the OD increment vs NaCl concentration.

(81) Sukhishvili, S. A.; Granick, S. *J. Am. Chem. Soc.* **2000**, *122*, 9550−9551.

(82) Shubin, V. *Langmuir* **1997**, *10*, 11093−11100. Akari, S.; Matthes, T.; Sommerhalter, C.; Boneberg, J.; Leiderer, P. *Langmuir* **1997**, *13*, 4369−4371. Qaqish, R. B.; Amiji, M. M. *Carbohydr. Polym.* **1999**, *38*, 99−107. Thuresson, K.; Lindman, B. *J. Phys. Chem. B* **1997**, *101*, 6460−6468. Ha, J. H.; Spolar, R. S.; Record, M. T., Jr. *J. Mol. Biol.* **1989**, *209*, 801−816.

(83) Israelashvili, J. *Intermolecular & Surface Forces*; Academic Press: London, 1992; pp 129−135.

(84) ζ-potential is the effective potential at the sheer surface of the ionic atmosphere, where ions forming the electric double layer start to move independently of the particle.

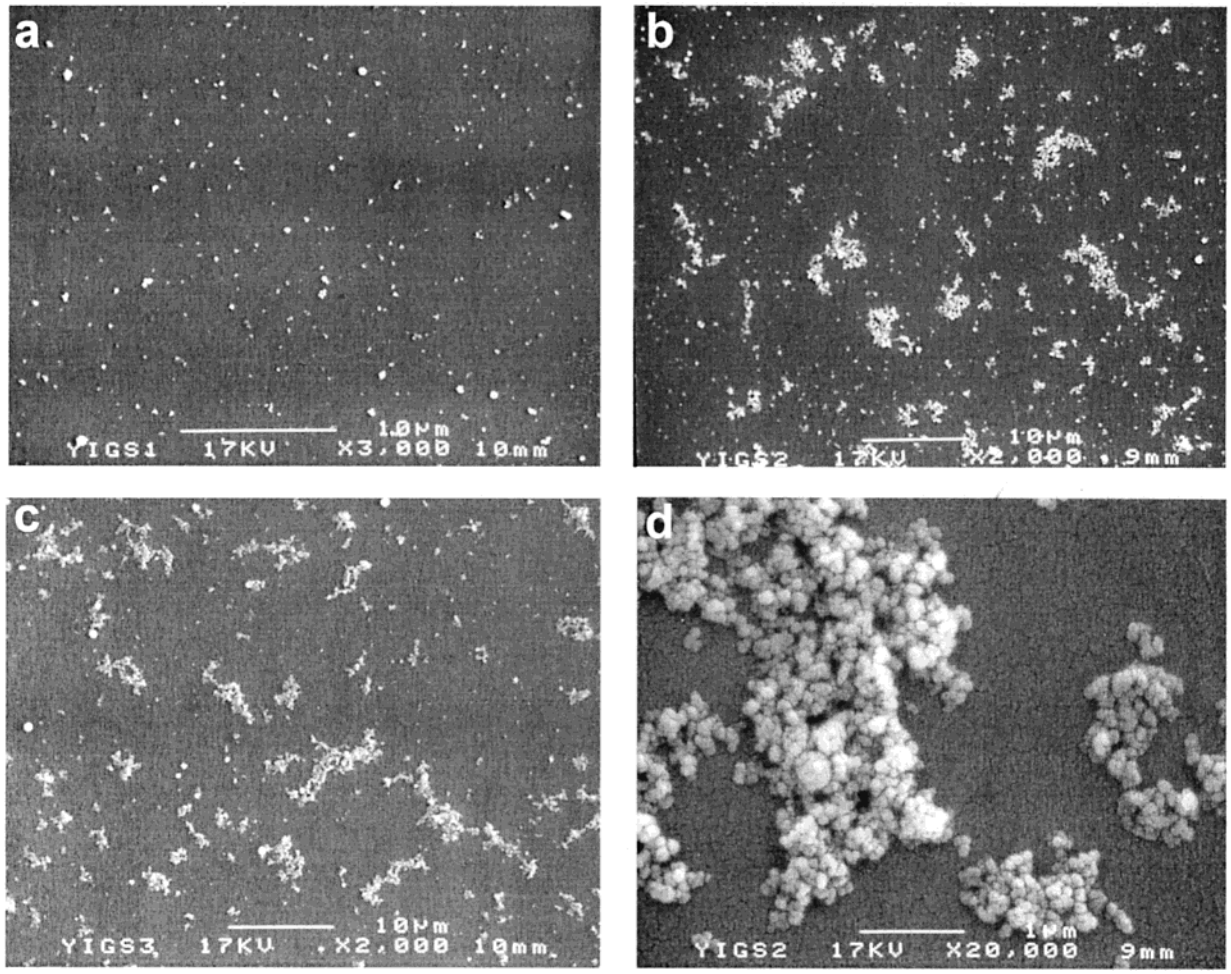

Figure 7. Scanning electron microscopy images of $(PDDA/YIG)_n$ films with (a) $n = 1$, (b and d) 2, and (c) 3 assembled from 0.2 M NaCl.

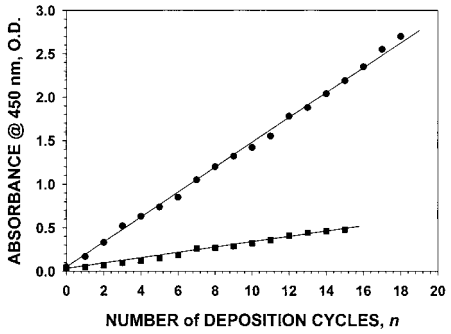

Figure 8. Dependence of optical density at 450 nm for the LBL assembly of the modified YIG (●) and nonmodified YIG (■) on the number of deposition cycles. A different wavelength than in Figures 2 and 8 was used to avoid reaching optical densities too high for measuring with a spectrophotometer.

hydrogen bonds.[81] However, we have not observed any isotope effect from replacing H_2O with D_2O on $\partial OD/\partial n$ and/or film morphology, which indicates that hydrogen bonds are unlikely to be the primary contributors to the assembly of modified YIG on polyelectrolytes.

Given the efficient adsorption of nanoparticles, one can further optimize the film structure. We found that the number of aggregates can be substantially reduced when carrying out the assembly of modified YIG on PAA at relatively low pH 2.9. A film with very uniform and dense packing of YIG nanoparticles has been obtained (Figure 10). The multilayer assemblies prepared at these conditions have excellent optical quality while also displaying strong magnetic properties, which is of significant interest for magnetooptical devices.[85] At low pH, the polyelectrolyte chains are not fully ionized and therefore are more compact than at high pH. It may be suggested that improved particle packing is related to the reduced tendency of weakly ionized polyelectrolytes to form loose loops and ends protruding from the surface into solution and serving as aggregation points for the nanoparticles, as was seen for the cross-linked polyelectrolyte molecules.[15]

Conclusions

The preparation of layered multifunctional assemblies from nanoparticles is important for both fundamental materials research and practical applications. Layer-by-layer assembly opens the way to the relatively easy and universal approach to the preparation of composite multilayer systems. In summary of this work, we want to emphasize two points, which appear to be the most significant for this research area: (1) LBL of nanoparticles can occur via two modes of deposition, which are difficult to recognize following the standard optical density vs number of layers plots. One of the modes allows for the preparation of the multilayer stacks (normal growth mode), while the other one does not (lateral expansion mode). (2) Film growth via the lateral expansion mode can be switched to the sandwich mode by organic modification of nanoparticles, which supplements the electrostatic interactions between nanoparticles and polymers with hydrophobic interactions.

(85) Murzina, T. V.; Nikulin, A. A.; Aktsipetrov, O. A.; Ostrander, J. W.; Mamedov, A. A.; Kotov, N. A.; Devillers, M. A. C.; Roark, J. *Appl. Phys. Lett.* **2000**, accepted for publication.

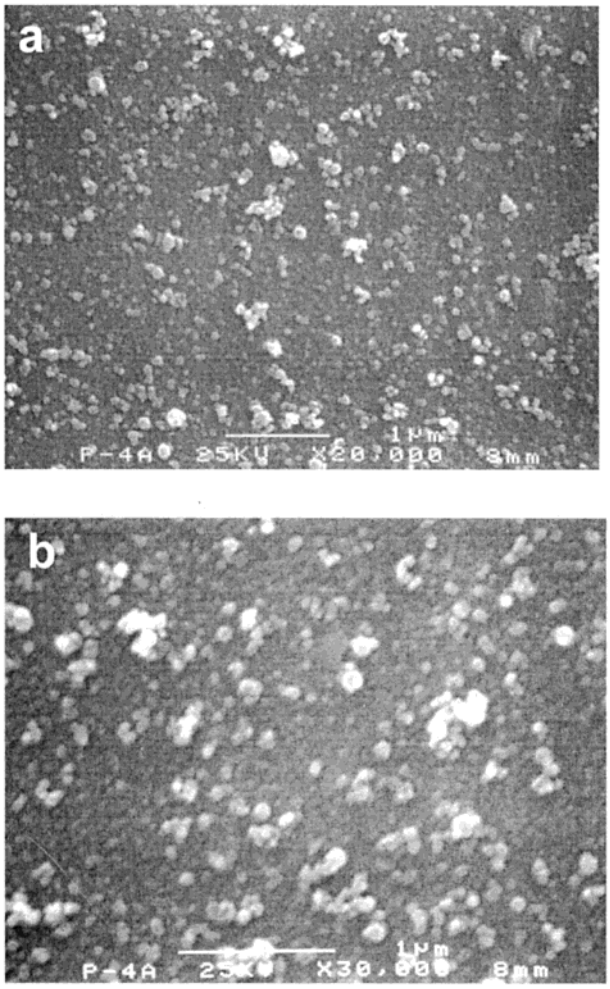

Figure 9. Scanning electron microscopy images of (PSS/modified YIG)$_n$ films with (a) $n = 1$ and (b) 2 assembled on a PDDA/PAA/PDDA precursor layer.

The bulk of this research is done with YIG nanoparticles as a model system, which affords preparation and assembly of both naked and modified nanoparticles unlike previously used nanoparticle dispersions. The evidence is also provided that the structural features observed for the PDDA/YIG LBL pair can also be seen for other colloids. These findings are important for understanding the interdependence of forces resulting in the layer-by-layer buildup, rational selection of the particle/polyelectrolyte systems, and control of the structure of the multilayer assemblies and photonic, electronic, magnetic, and biological materials based on them.

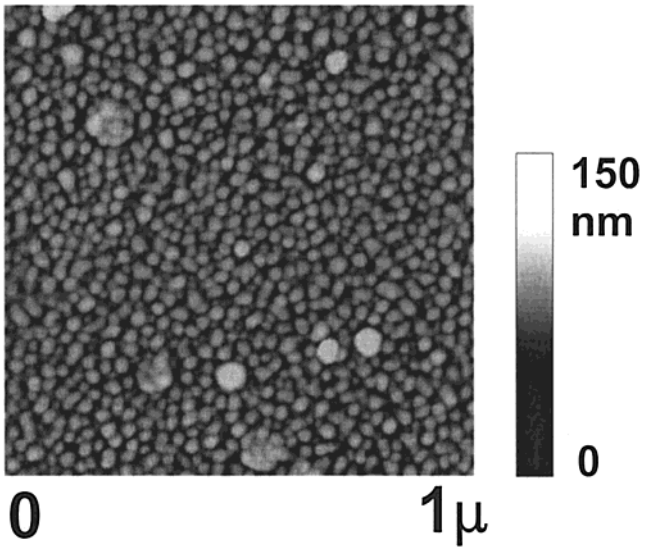

Figure 10. Atomic force microscopy image of a (PAA/modified YIG)$_1$ film assembled on a PDDA/PAA/PDDA precursor layer.

Acknowledgment. The authors thank Drs. O. Aktsipetrov and T. Murzina from the Department of Physics, Moscow State University, Moscow, Russia for their help with ellipsometric measurements and fruitful discussions. N.A.K. thanks NSF CAREER (CHE-9876265), AFOSR (F49620-99-C-0072), NATO (CRG 971167), OSU Sensor Center, OSU Center for Laser and Photonics Research, and Nomadics Inc. for the financial support of this research. N.A.K. also thanks all members of the research group in OSU for their dedicated work on LBL and other projects and referees for helpful comments on the manuscript.

Supporting Information Available: Figure showing the atomic force microscopy images of PDDA/YIG (PDF). This material is available free of charge via the Internet at http://pubs.acs.org.

JA0029578